

COMMUNICATION

Light driven water oxidation by a single site cobalt salophen catalyst†

Cite this: *Chem. Commun.*, 2013, **49**, 9941

Received 18th July 2013,
Accepted 30th August 2013

DOI: 10.1039/c3cc45457f

www.rsc.org/chemcomm

A salophen cobalt(II) complex enables water oxidation at neutral pH in photoactivated sacrificial cycles under visible light, thus confirming the high appeal of earth abundant single site catalysis for artificial photosynthesis.

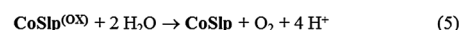
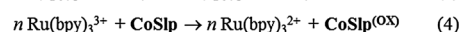
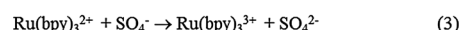
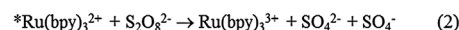
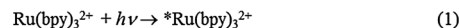
Inspired by the natural Mn_4CaO_x oxygen evolving centre in photosystem II,¹ remarkable efforts have been dedicated towards the development of multinuclear transition metal complexes enabling water oxidation for artificial photosynthesis.^{2,3} Multi-metallic catalysts could in principle distribute the oxidation equivalents necessary for water oxidation over several metal centres, thus lowering the energy barrier of the overall catalytic process.³ However, the design of multi-metallic cores with oxygen evolving activity poses synthetic and stability hurdles.³

Noteworthy, single site metal complexes have been recently discovered, whose oxygen evolving activity offers a major opportunity to broaden the catalyst space within fundamental coordination chemistry.⁴ Of particular interest are the earth-abundant cobalt complexes featuring polydentate organic ligands, such as corroles, polypyridines, porphyrins, and polyamines, which have been used under dark electrocatalysis conditions,⁵ and in few cases also within photoactivated cycles.⁶ Ligand diversity is expected to play a crucial role in tuning photocatalytic water oxidation, with the urgent quest to both optimize sequential photoinduced electron transfer and facilitate the dark-phase of the catalytic mechanism under a turnover regime.

Erica Pizzolato,^a Mirco Natali,^b Bianca Posocco,^a Alejandro Montellano López,^a Irene Bazzan,^a Marilena Di Valentin,^a Pierluca Galloni,^c Valeria Conte,^c Marcella Bonchio,^a Franco Scandola*^b and Andrea Sartorel*^a



CoSlp



Scheme 1 Photoactivated water oxidation in the $\text{Ru}(\text{bpy})_3^{2+}/\text{S}_2\text{O}_8^{2-}$ system catalysed by **CoSlp**.

In this communication we present a cobalt(II) complex with a salophen ligand (*N,N'*-bis(salicylaldehyde)-1,2-phenylenediamine), **CoSlp**, capable of water oxidation under visible light irradiation, with $\text{Ru}(\text{bpy})_3^{2+}$ ($\text{bpy} = 2,2'$ -bipyridine) as the photosensitizer and persulfate ($\text{S}_2\text{O}_8^{2-}$) as the sacrificial electron acceptor (Scheme 1). Combined UV-vis, dynamic light scattering (DLS) and Electron Paramagnetic Resonance (EPR) evidence identifies **CoSlp** as a competent oxygen evolving catalyst (OEC), enabling a two-fold photoinduced electron transfer in the ms time-frame. Our results confirm the “privileged” nature of the salophen ligand environment, readily available from simple condensation reactions, with wide applicability in different fields of catalysis, including bio-inspired oxidations.⁷

CoSlp is obtained by direct reaction of cobalt acetate with the salophen ligand in methanol, followed by precipitation with diethyl ether and recrystallization.^{8†} Its solid state and solution identity was initially verified using FT-IR and UV-vis spectroscopy through comparison with literature data (Fig. S2 and S3, ESI†),⁸ then confirmed using ESI-MS, where a base peak at $m/z = 374$ was observed, ascribed to the $[\text{CoSlp}\cdot\text{H}]^+$ ion (Fig. S4, ESI†). In the solid state, the cobalt ion in **CoSlp** displays a square planar geometry,^{8c} while in aqueous solution it extends the coordination sphere to square pyramidal, by ligation of a water molecule in the apical position.^{8d} Spectrophotometric titration yields a $\text{p}K_a = 6.40$ for the aquo ligand (Fig. S5, ESI†),⁹ which is therefore expected to be deprotonated at neutral pH, turning into a hydroxo moiety.

Characterisation of **CoSlp** by cyclic voltammetry in aqueous phosphate buffer at pH 7.1 shows the onset of an intense anodic wave beginning at ca. 0.90 V (vs. Ag/AgCl) reaching a peak current of

^a ITM-CNR and Department of Chemical Sciences, University of Padova, via Marzolo 1, 35131 Padova, Italy. E-mail: andrea.sartorel@unipd.it; Fax: +39 049 8275330; Tel: +39 049 8275252

^b Department of Chemical and Pharmaceutical Sciences, University of Ferrara, and Centro Interuniversitario per la Conversione Chimica dell'Energia Solare (sez. Ferrara), via Fossato di Mortara 17-27, 44121 Ferrara, Italy. E-mail: snf@unife.it; Fax: +39 0532 240709; Tel: +39 0532 455160

^c Department of Chemical Sciences and Technologies, University of Rome Tor Vergata, via della Ricerca Scientifica, 00133 Roma, Italy

† Electronic supplementary information (ESI) available: Synthesis and full characterization of **CoSlp**, experimental procedures for cyclic voltammeteries, oxygen evolving experiments, quantum yield determination, laser flash photolysis, and EPR. See DOI: 10.1039/c3cc45457f

250 μA (current density of 3.5 mA cm^{-2}) at 1.35 V (Fig. S6, ESI[†]). The attribution of this intense wave to catalytic water oxidation was supported by the presence of a cathodic wave at -230 mV , observed only in the reverse scan, due to reduction of dioxygen formed at the working electrode (Fig. S6, ESI[†]).^{8b} Although electrodeposited heterogeneous cobalt oxide can possibly plague the voltammetric analysis,¹⁰ † the electrochemical study allows for some key observations, namely:

–a marked difference in the **CoSlp** voltammogram with respect to the “ligand-free” cobalt aquo complex, known to evolve into electrodeposited oxide phases upon application of an anodic bias,^{10b}

–an increase of the normalized current (defined as the current divided by the square root of the scan rate) at low scan rates which confirms the presence of a rate determining chemical step preceding electron transfer (Fig. S6, ESI[†]);^{5c,11}

–a very low operating overpotential, $\eta = 0.3 \text{ V}$ at 0.7 mA cm^{-2} current density, which outperforms previously reported cobalt OECs, with overpotentials in the range $0.5\text{--}0.6 \text{ V}$.⁵

This latter observation is pivotal to light-driven water oxidation under homogeneous conditions, usually achieved in the presence of a photosensitizer and a sacrificial electron acceptor, respectively, $\text{Ru}(\text{bpy})_3^{2+}$ and $\text{S}_2\text{O}_8^{2-}$ in the present case (eqn (1)–(5) in Scheme 1).³ In such a system, the photogenerated oxidant is the $\text{Ru}(\text{bpy})_3^{3+}$ species, produced by reaction of the excited state of $\text{Ru}(\text{bpy})_3^{2+}$ with the persulfate anion (eqn (1)–(3)). The $\text{Ru}(\text{bpy})_3^{3+}$ then oxidizes the catalyst **CoSlp** to an activated form, generally indicated as **CoSlp**^(OX) (eqn (4)), which is capable of oxidizing water to oxygen restoring the initial state of the catalyst (eqn (5)).³

The photosynthetic activity of **CoSlp** ($15\text{--}125 \mu\text{M}$) was confirmed by oxygen evolution upon illumination of a 20 mM phosphate buffered aqueous solution ($\text{pH } 7$) containing 1 mM $\text{Ru}(\text{bpy})_3^{2+}$ and 5 mM $\text{S}_2\text{O}_8^{2-}$ (Fig. 1a). An initial lag-time is observed in the kinetic traces, due to accumulation of a steady-state concentration of the photogenerated intermediates, as it is eliminated by increasing the irradiation flux. The maximum turnover rate and the total amount of oxygen produced depend on the catalyst concentration, showing a saturation-inhibition behavior for $[\text{CoSlp}] > 100 \mu\text{M}$ (Fig. 1a and Table S1, ESI[†]). The oxygen production levels off after *ca.* 2 hours due to $\text{Ru}(\text{bpy})_3^{2+}$ degradation, as revealed by the partial bleaching of the absorption at 450 nm (Fig. S7, ESI[†]). In this timeframe, **CoSlp** operates for up to 17 turnovers. The most significant parameter to describe the performance of a photoactivated system is the quantum yield (Φ_{O_2}),³ defined as the ratio between the oxygen produced and the photons absorbed by the system (eqn (6)).

$$\Phi_{\text{O}_2} = \frac{\text{O}_2 \text{ produced}}{\text{absorbed photons}} \quad (6)$$

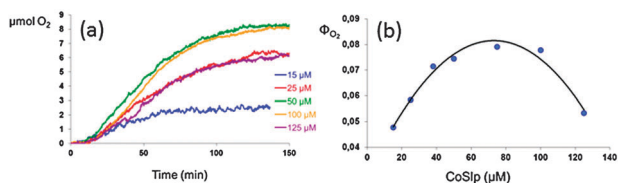


Fig. 1 (a) Representative kinetics of O_2 evolution in the photoactivated system, $[\text{CoSlp}] = 15\text{--}125 \mu\text{M}$, $[\text{Ru}(\text{bpy})_3^{2+}] = 1 \text{ mM}$, $[\text{S}_2\text{O}_8^{2-}] = 5 \text{ mM}$ in 20 mM phosphate buffer, $\text{pH } 7$; illumination by LED emission at 450 nm , see ESI[†]. (b) Φ_{O_2} of the process versus **CoSlp** concentration.

Under the explored conditions, Φ_{O_2} was found in the range $0.048\text{--}0.079$, corresponding to $9.6\text{--}15.8\%$ efficiency in photon to O_2 conversion,[§] with a bell-shaped profile depending on **CoSlp** concentration (Fig. 1b). A similar bell-shaped profile was already observed with a tetracobalt cubane catalyst,¹² and abatement of the rate of O_2 production at $>100 \mu\text{M}$ cobalt concentration was indeed noted also with other molecular precatalysts.^{6c} This behavior is related to competitive unproductive routes amplified at high catalyst concentration, and likely identifiable with quenching of the $\text{Ru}(\text{bpy})_3^{2+}$ excited state by **CoSlp** and by its intermediates involved in the catalytic cycle.

In photoactivated cycles devoted to oxygen production, a critical step that often determines the overall efficiency is the electron transfer rate from the catalyst to the oxidized photosensitizer (eqn (4) in Scheme 1).^{3,13} This can be conveniently investigated by performing laser flash photolysis experiments, where a suitable concentration of $\text{Ru}(\text{bpy})_3^{3+}$ is generated in a $<10 \text{ ns}$ timeframe by 355 nm laser activated reaction of $\text{Ru}(\text{bpy})_3^{2+}$ with $\text{S}_2\text{O}_8^{2-}$ (eqn (1)–(3)), while the following reaction of $\text{Ru}(\text{bpy})_3^{3+}$ with **CoSlp** is monitored in a ms timescale by the recovery of the absorption at 450 nm , due to $\text{Ru}(\text{bpy})_3^{2+}$ regeneration (Fig. 2). As shown in Fig. 2a, the rate of recovery of the absorption of $\text{Ru}(\text{bpy})_3^{2+}$ at 450 nm depends on **CoSlp** concentration,[¶] and assuming pseudo-first order kinetic conditions, a bimolecular rate constant of $1.12 \times 10^8 \text{ M}^{-1} \text{ s}^{-1}$ is obtained for the first electron transfer event (Fig. S8, ESI[†]), likely involving the formation of a $\text{Co}(\text{IV})$ intermediate. This value is one order of magnitude higher with respect to a tetracobalt cubane catalyst, explored under the same conditions.¹²

Moreover, examination of the process with sub-stoichiometric catalyst solutions^{13a} shows that each **CoSlp** is able to scavenge *ca.* two $\text{Ru}(\text{bpy})_3^{3+}$ within a time window of 40 ms (Fig. 2b). This suggests the fast formation of a formal $\text{Co}(\text{IV})$ derivative by two consecutive one-electron oxidation of **CoSlp** by $\text{Ru}(\text{bpy})_3^{3+}$ under irradiation conditions. A possible mechanistic scenario foresees the involvement of a photogenerated $\text{Co}(\text{IV})$ -oxo intermediate,^{||} undergoing a rate determining nucleophilic attack¹⁴ by a water molecule. A new oxygen–oxygen bond is then formed, within the structural motif of $\text{Co}(\text{II})$ -hydroperoxide (Scheme 2); such an intermediate could finally release O_2 upon further oxidation.^{5b,c,14,15}

As a final remark, stability is a major requirement in order to consider a catalyst for potential application in regenerative oxygen evolving photoanodes.³ In the present case, UV-vis experiments reveal unchanged absorption spectra over several hours of **CoSlp** in 20 mM aqueous phosphate buffer ($\text{pH } 7$), also in the presence of the persulfate anion. Under photocatalytic conditions, dynamic light scattering analysis of the reaction mixtures yields no evidence of any

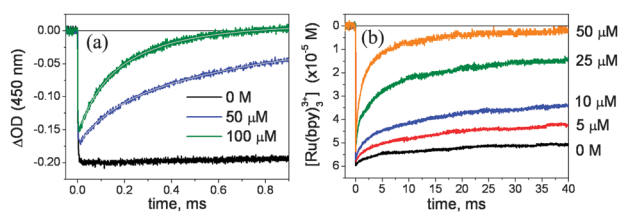
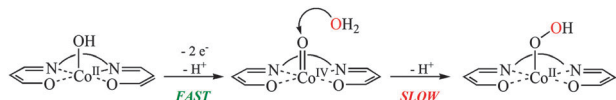


Fig. 2 Laser flash photolysis experiments ($\lambda_{\text{exc}} = 355 \text{ nm}$) in aqueous phosphate buffer ($\text{pH } 7$) containing 5 mM $\text{S}_2\text{O}_8^{2-}$ and: (a) $50 \mu\text{M}$ $\text{Ru}(\text{bpy})_3^{2+}$, $0\text{--}100 \mu\text{M}$ **CoSlp**; (b) $100 \mu\text{M}$ $\text{Ru}(\text{bpy})_3^{2+}$, $0\text{--}50 \mu\text{M}$ **CoSlp**.



Scheme 2 Possible reaction route leading to oxygen–oxygen bond formation in the photocatalytic cycle.

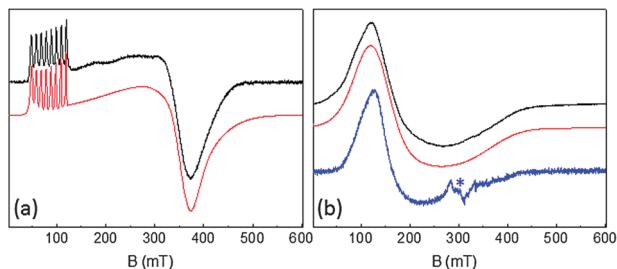


Fig. 3 X-band CW-EPR experimental spectra at 10 K and corresponding simulations (in red) of **CoSlp**: (a) 1 mM in CH_2Cl_2 : CH_3OH 9:1; (b) black trace: 1 mM in CH_3CN :phosphate buffer (20 mM, pH 7) 1:1; blue trace: 0.5 mM in CH_3CN :phosphate buffer (20 mM, pH 7) 1:1 containing 1 mM $\text{Ru}(\text{bpy})_3^{2+}$ and 5 mM $\text{S}_2\text{O}_8^{2-}$ after 1 h illumination. * Cavity artefact.

dispersion, suggesting the absence of Co-oxide colloids.^{6b} Moreover, the reaction mixture has been analysed using X-band continuous-wave (CW) EPR spectroscopy (Fig. 3). When frozen in a CH_2Cl_2 : CH_3OH 9:1 matrix, **CoSlp** shows an orthorhombic EPR spectrum at 10 K with $g_1 = 7.90$, $g_2 = 1.90$ and $g_3 = 1.85$, where the signal due to the highest g component shows an eight-line cobalt-hyperfine splitting ($A_1 = 1100$ MHz, Fig. 3a). According to spectral simulation this is consistent with a $S = 3/2$ species, as expected for a d^7 high spin configuration of the Co(II) ion.^{8d,16} In the aqueous phase (CH_3CN :phosphate buffer 1:1), the EPR spectrum is characterised by the presence of a featureless and nearly axial signal with g values of $g_1 = 4.95$, $g_2 = 3.75$ and $g_3 = 2.05$ (black trace in Fig. 3b), which is still assigned to an $S = 3/2$ Co(II) species.¹⁷ The occurrence of a high-spin Co(II) signal is likely due to strong axial interactions and/or distortions of the planar structure of the complex in both media.^{8d,16b,17,18} Under photocatalytic conditions, the EPR spectrum obtained for **CoSlp** does not undergo major changes even after prolonged illumination in the presence of $\text{Ru}(\text{bpy})_3^{2+}$ and $\text{S}_2\text{O}_8^{2-}$ (blue trace in Fig. 3b). No signals of free Co(II) ions or Co(III) oxides are detectable,^{16,19} thus confirming the resting form of **CoSlp** and its stability under the operating conditions.

In conclusion, we have presented a novel molecular water oxidation catalyst, based on a single site cobalt salophen complex. This species catalyses water oxidation in neutral aqueous medium electrochemically and in a photoactivated system, showing very high electron transfer rates to the photo-generated oxidant $\text{Ru}(\text{bpy})_3^{3+}$. Structure reactivity studies,²⁰ by introducing substituents in the aromatic rings of the catalyst, will be addressed to optimize catalyst performance.

COST Action CM1003 “Biological oxidation reactions – mechanisms and design of new catalysts” is gratefully acknowledged. This work was supported by the Italian MIUR (FIRB “Nano-Solar” RBAP11C58Y, PRIN “Hi-Phuture” 2010N3T9M4_001), the University of Padova (PRAT CPDA104105/10 and 2008 HELIOS project STPD08RCX), and Fondazione Cariparo (Nanomode,

progetti di eccellenza 2010). We thank Laura Meneghini for EPR simulations.

Notes and references

‡ The residual presence of an anodic wave, with *ca.* 30% intensity of the pristine curve, in a **CoSlp**-free solution, with an unpolished working electrode from a previous scan indicates the possible absorption–deposition of active material onto the working electrode.^{5b,c}

§ In $\text{Ru}(\text{bpy})_3^{2+}$ - $\text{S}_2\text{O}_8^{2-}$ systems, the maximum value of Φ_{O_2} is indeed 0.5, since two $\text{Ru}(\text{bpy})_3^{3+}$ are possibly generated upon absorption of one photon (eqn (1)–(3)), and at least four $\text{Ru}(\text{bpy})_3^{3+}$ are required to produce one O_2 molecule.³ Reported quantum efficiencies for a single site Co precatalyst reach up to 30%.^{6c}

¶ The decrease in the initial ΔOD observed upon **CoSlp** addition is mainly attributed to laser absorption by **CoSlp** and quenching of $^*\text{Ru}(\text{bpy})_3^{2+}$ by the cobalt catalyst (Fig. S9, ESI†).

|| Co(IV)-oxo species may display a spin distribution on the oxygen atom, and therefore should be better described as Co(III)- $\text{O}^{\bullet-}$ (Co-oxyl).¹⁵

- 1 Y. Umena, K. Kawakami, J.-R. Shen and N. Kamiya, *Nature*, 2011, **473**, 55.
- 2 *Faraday Disc.*, 2012, **155**, 1–388, themed issue Artificial Photosynthesis.
- 3 A. Sartorel, M. Bonchio, S. Campagna and F. Scandola, *Chem. Soc. Rev.*, 2013, **42**, 2262.
- 4 (a) D. J. Wasylenko, R. D. Palmer and C. P. Berlinguette, *Chem. Commun.*, 2013, **49**, 218; (b) D. G. H. Hetterscheid and J. N. H. Reek, *Angew. Chem., Int. Ed.*, 2012, **51**, 9740.
- 5 (a) D. K. Dogutan, R. McGuire Jr. and D. G. Nocera, *J. Am. Chem. Soc.*, 2011, **133**, 9178; (b) D. J. Wasylenko, C. Ganesamoorthy, J. Borau-Garcia and C. P. Berlinguette, *Chem. Commun.*, 2011, **47**, 4249; (c) D. J. Wasylenko, R. D. Palmer, E. Schott and C. P. Berlinguette, *Chem. Commun.*, 2012, **48**, 2107.
- 6 (a) C.-F. Leung, S.-M. Ng, C.-C. Ko, W.-L. Man, J. Wu, L. Chen and T.-C. Lau, *Energy Environ. Sci.*, 2012, **5**, 7903; (b) T. Nakazono, A. R. Parent and K. Sakai, *Chem. Commun.*, 2013, **49**, 6325; (c) D. Hong, J. Jung, J. Park, Y. Yamada, T. Suenobu, Y.-M. Lee, W. Nam and S. Fukuzumi, *Energy Environ. Sci.*, 2012, **5**, 7606.
- 7 P. G. Cozzi, *Chem. Soc. Rev.*, 2004, **33**, 410.
- 8 (a) A. Pui, C. Dobrota and J. P. Mahy, *J. Coord. Chem.*, 2007, **60**, 581; (b) B. Ortiz and S. M. Park, *Bull. Korean Chem. Soc.*, 2000, **21**, 405; (c) N. B. Pahor, M. Calligaris, P. Delise, G. Dodic, G. Nardin and L. Randaccio, *J. Chem. Soc., Dalton Trans.*, 1976, 2478; (d) B. J. Kennedy, G. D. Fallon, B. M. K. C. Gatehouse and K. S. Murray, *Inorg. Chem.*, 1984, **23**, 580.
- 9 C. A. Ohlin, S. J. Harley, J. G. McAlpin, R. K. Hocking, B. Q. Mercado, R. L. Johnson, E. M. Villa, M. K. Fidler, M. M. Olmstead, L. Spiccia, R. D. Britt and W. H. Casey, *Chem.–Eur. J.*, 2011, **17**, 4408.
- 10 (a) J. J. Stracke and R. G. Finke, *J. Am. Chem. Soc.*, 2011, **133**, 14872; (b) M. W. Kanan and D. G. Nocera, *Science*, 2008, **321**, 1072.
- 11 Z. Chen, J. J. Concepcion, H. Luo, J. F. Hull, A. Paul and T. J. Meyer, *J. Am. Chem. Soc.*, 2010, **132**, 17670.
- 12 G. La Ganga, F. Puntoriero, S. Campagna, I. Bazzan, S. Berardi, M. Bonchio, A. Sartorel, M. Natali and F. Scandola, *Faraday Discuss.*, 2012, **155**, 177.
- 13 (a) M. Natali, M. Orlandi, S. Berardi, S. Campagna, M. Bonchio, A. Sartorel and F. Scandola, *Inorg. Chem.*, 2012, **51**, 7324; (b) M. Natali, S. Berardi, A. Sartorel, M. Bonchio, S. Campagna and F. Scandola, *Chem. Commun.*, 2012, **48**, 8808.
- 14 Z. Chen, J. J. Concepcion, X. Hu, W. Yang, P. G. Hoertz and T. J. Meyer, *Proc. Natl. Acad. Sci. U. S. A.*, 2010, **107**, 7225.
- 15 M. Z. Ertem and C. J. Cramer, *Dalton Trans.*, 2012, **41**, 12213.
- 16 (a) E. Vinck, D. M. Murphy, I. A. Fallis and S. Van Doorslaer, *Appl. Magn. Reson.*, 2010, **37**, 289; (b) B. Bennett and R. C. Holz, *J. Am. Chem. Soc.*, 1997, **119**, 1923.
- 17 E. Vinck, E. Carter, D. M. Murphy and S. Van Doorslaer, *Inorg. Chem.*, 2012, **51**, 8014.
- 18 C. Daul, C. W. Schläpfer and A. von Zelewsky, *Struct. Bonding*, 1979, **36**, 129.
- 19 J. G. McAlpin, Y. Surendranath, M. Dincă, T. A. Stich, S. A. Stoian, W. H. Casey, D. G. Nocera and R. D. Britt, *J. Am. Chem. Soc.*, 2010, **132**, 6882.
- 20 (a) S. Berardi, G. La Ganga, M. Natali, I. Bazzan, F. Puntoriero, A. Sartorel, F. Scandola, S. Campagna and M. Bonchio, *J. Am. Chem. Soc.*, 2012, **134**, 11104; (b) Z. Codola, I. Garcia-Bosch, F. Acuña-Parés, I. Prat, J. M. Luis, M. Costas and J. Lloret-Fillol, *Chem.–Eur. J.*, 2013, **19**, 8042.